

RESEARCH ARTICLE | MARCH 06 2024

Low-frequency whistler waves driven by energetic electrons in plasmas of solely electron cyclotron wave heating

Mingyuan Wang ; Yuejiang Shi ; Jiaqi Dong  ; Xinliang Gao ; Quanming Lu ; Ziqi Wang; Wei Chen; Adi Liu ; Ge Zhuang ; Yumin Wang ; Shikui Cheng ; Mingsheng Tan; Songjian Li ; Shaodong Song; Tiantian Sun; Bing Liu; Xianli Huang ; Yingying Li ; Xianming Song; Baoshan Yuan; Y.-K. Martin Peng 

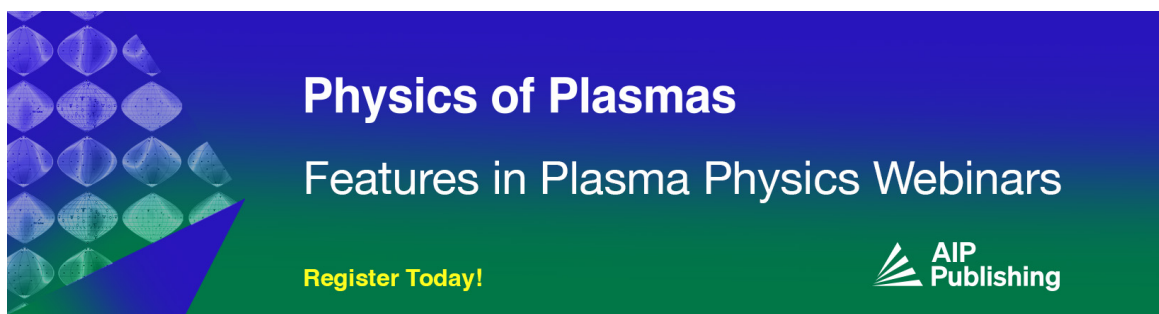


Phys. Plasmas 31, 032105 (2024)

<https://doi.org/10.1063/5.0195750>




CrossMark



Physics of Plasmas
Features in Plasma Physics Webinars

Register Today!



Low-frequency whistler waves driven by energetic electrons in plasmas of solely electron cyclotron wave heating

Cite as: Phys. Plasmas **31**, 032105 (2024); doi: 10.1063/5.0195750

Submitted: 4 January 2024 · Accepted: 12 February 2024 ·

Published Online: 6 March 2024



View Online



Export Citation



CrossMark

Mingyuan Wang,^{1,2,3} Yuejiang Shi,^{2,3,a)} Jiaqi Dong,^{2,3,a)} Xinliang Gao,⁴ Quanming Lu,⁴ Ziqi Wang,^{2,3} Wei Chen,⁵ Adi Liu,⁴ Ge Zhuang,⁴ Yumin Wang,^{2,3} Shikui Cheng,^{2,3,5} Mingsheng Tan,⁶ Songjian Li,^{2,3} Shaodong Song,^{2,3} Tiantian Sun,^{2,3} Bing Liu,^{2,3} Xianli Huang,^{2,3} Yingying Li,^{2,3} Xianming Song,^{2,3} Baoshan Yuan,^{2,3} and Y.-K. Martin Peng^{2,3}

AFFILIATIONS

¹School of Mathematics and Physics, Anqing Normal University, Anqing 246133, People's Republic of China

²Hebei Key Laboratory of Compact Fusion, Langfang 065001, China

³ENN Science and Technology Development Co., Ltd., Langfang 065001, China

⁴University of Science and Technology of China, Anhui, Hefei 230026, China

⁵Southwestern Institute of Physics, Chengdu 610041, China

⁶Institute of Energy, Hefei Comprehensive National Science Center, Hefei 230031, China

^{a)} Authors to whom correspondence should be addressed: yjshi@ipp.ac.cn and jiaqi@swip.ac.cn

ABSTRACT

Whistler waves are a type of low-frequency electromagnetic wave common in nature, which is usually associated with energetic electron phenomena. This study presents experimental observations of low-frequency whistler wave instabilities driven by energetic electrons through wave-particle interactions on EXL-50. The energetic electrons are generated by electron cyclotron waves (ECWs) through stochastic heating [Wang *et al.*, *J. Plasma Phys.* **89**, 905890603 (2023)] and do not match the characteristics of the runaway electrons [Shi *et al.*, *Nucl. Fusion* **62**, 086047 (2022)]. In the steady-state plasma of the Energy iNnovation XuanLong-50 (EXL-50), whistler waves within the 30–120 MHz frequency range were observed during electron cyclotron resonance heating. These waves displayed multiple frequency bands, and the frequencies of waves were directly proportional to the Alfvén velocity. Furthermore, it was interesting to find that superposition of lower hybrid wave into ECW resulted in the suppression of these whistler waves. The experimental results may indicate that the whistler waves are driven by energetic electrons (excluding runaway electrons). These discoveries carry significant implications for several areas of research, including the investigation of wave-particle interactions, the development of radio frequency wave current drivers, their potential impact on the electron dynamics in future fusion devices, and even the presence of unusually low-frequency whistler waves in Earth's radiation belts.

Published under an exclusive license by AIP Publishing. <https://doi.org/10.1063/5.0195750>

INTRODUCTION

Whistler waves, as fundamental plasma waves, have been widely observed in space and laboratory plasma, which have the potential to affect the electron dynamics. It is widely accepted that the wave-particle interaction with whistler waves is the dominant mechanism for energizing electrons in the radiation belt.^{1–4}

The whistler wave occurring in the frequency (ω) range of 0.1 to 0.8 times the electron cyclotron frequency (ω_{ce}) is commonly observed in the outer radiation belt. Additionally, unusually low frequency whistler wave ($\omega < 0.1\omega_{ce}$) has also observed in the outer radiation belt.^{5,6} Research by Xiao *et al.*⁷ suggests that the presence of electrons with an

energetic tail population and relativistic pitch angle anisotropy can supply the requisite free energy for generating whistler waves below $0.1\omega_{ce}$.

In laboratory experiments, whistler waves have been excited using methods, such as electron beams, whistler wave antennas, and runaway electrons.^{3,8–17} Low frequency whistler waves ($\omega < 0.1\omega_{ce}$) driven by runaway electrons of parallel temperature (T_{\parallel}) higher than perpendicular temperature (T_{\perp}) have been observed in various tokamaks.^{15–17}

Fülöp and colleagues conducted a comprehensive investigation on relativistic electron beam-driven whistler waves.¹⁸ Their research

work emphasizes the ability of the runaway electron beam to drive low-frequency whistler waves. Subsequently, the dispersion relation of these whistler waves was measured using fast wave antennas in DIII-D experiments,^{15–17} confirming the finding of Fülöp's work. Additionally, the presence of whistler waves was found to enhance electron cyclotron emission (ECE) signals, potentially due to the pitch angle scattering of runaway electrons by the whistler waves. This discovery offers a potential method to mitigate the threat posed by runaway electrons.

Liu *et al.* conducted a theoretical study on the influence of the kinetic whistler wave instability on the runaway electrons avalanche.^{19,20} The runaway electron avalanche refers to a phenomenon where a small number of energetic electrons in plasma gain additional energy and subsequently collide with other electrons, transferring energy and causing a cascading effect that leads to a significant increase in the number of energetic runaway electrons.²¹ Their study revealed that under high-density and low-electric-field conditions, whistler wave scattering can effectively suppress the avalanche and increase the threshold electric field required for the avalanche to occur.

Guo *et al.* proposed a novel approach to mitigate the harm caused by runaway electrons by limiting their energy to less than a few MeV through the external injection of whistler waves.²² This research indicates that the whistler waves resonate with runaway electrons within a specific energy range, effectively altering the momentum-space vortex of the runaway electrons. The scattering of whistler waves can reshape the vortex by cutting off highly relativistic electrons, thus reducing the upper limit of energetic electrons.

In this study, we present the first experimental observation of whistler wave instability driven by energetic electrons in ECW-only steady-state plasma. These observations, conducted on a steady-state operating experimental platform, provide valuable insight into the physical mechanisms of wave-particle interaction and have important implications for understanding the ionosphere of the Earth, Van Allen belts, and tokamak reactors.

First, this paper reports on high frequency mode excitation experiments conducted on the Energy iNnovation XuanLong-50 (EXL-50) spherical torus and presents the main characteristics of the mode in steady-state ECW plasma. The experimental results showed that the mode frequencies were found to be greater than the ion cyclotron frequency (ω_{ci}) but much smaller than ω_{ce} . Additionally, it was observed that the mode frequencies were proportional to the Alfvén velocity (V_A) and that the mode featured multiple frequency bands. These findings suggest that these modes are low frequency whistler waves, which are driven by energetic electrons.^{2,18} Moreover, the energetic electrons being generated by electron cyclotron waves (ECWs) through stochastic heating have been demonstrated on the EXL-50,²³ and these energetic electrons do not match the characteristics of the runaway electrons.²⁴

A lower-hybrid wave (LHW), which was used to increase the electron parallel velocity, resulted in significant whistler wave suppression. Additionally, it is worth noting that disruptions associated with whistler waves were observed, which implies that these waves may trigger magnetic re-connection.^{25–27} These studies contribute to the understanding of whistler wave physics in tokamaks and provide valuable insight for the research on RF current drive and control of runaway electrons.

EXL-50 EXPERIMENT SETUP

The whistler wave experiments were performed on the EXL-50 spherical torus using ECWs at 28 GHz with a power of approximately 200 kW and LHW at 2.45 GHz with a power of approximately 60 kW in low electron density plasma (the line integrated density $n_{el} \sim 1\text{--}2 \times 10^{18} \text{ m}^{-2}$).²⁸ EXL-50 is a medium-sized spherical torus without a central solenoid (CS), featuring a major 0.58 m, a minor radius of approximately 0.41 m, a toroidal magnetic field (B_T) of approximately 0.5 T at $R \sim 0.48$ m, and an aspect ratio of $A > 1.45$. Unless otherwise specified, only the ECW was used to heat and maintain the plasma. A large number of energetic electrons are generated by the ECW²³ to startup²⁹ and maintain plasma currents.²⁴ The whistler wave fluctuations, associated with sufficient anisotropy of the electron velocity distribution (especially energetic electrons), may be excited,^{2,10,30,31} and measured using a high-frequency magnetic probe on the low field-side of the mid-plane³² (as illustrated in Fig. 1). The energetic electron loss to the wall was measured using CdZnTe detectors and a LaBr3(Ce) scintillation hard x-ray detector.³³ The LaBr3(Ce) scintillation detector was placed approximately 20 m away from the torus center.

In previous experiments,^{23,24} the hard x-ray (HXR) detectors with improved lead shielding are applied. Beside the original shielding (10 mm lead +5 mm steel),³³ the CdZnTe detectors have their own independent 50 mm lead shielding. Through this improved shielding HXR system, it has been experimentally verified that the ECW generates energetic electrons through a stochastic heating mechanism.²³ Moreover, based on a simplified three-temperature radiation model, the parallel and vertical temperatures and intensity of energetic electrons were calculated to be similar level.²⁴ These results suggest that the energetic electrons in EXL-50 are not runaway electrons.

Subsequently, the independent 50 mm lead shielding of the detectors was discarded following an upgrade of the EXL-50 device in recent experiment campaign. The HXR system mainly measure thick-target radiation resulting from energetic electrons losses at the wall because of remove of the lead shielding. As shown in Fig. 2, only ECW

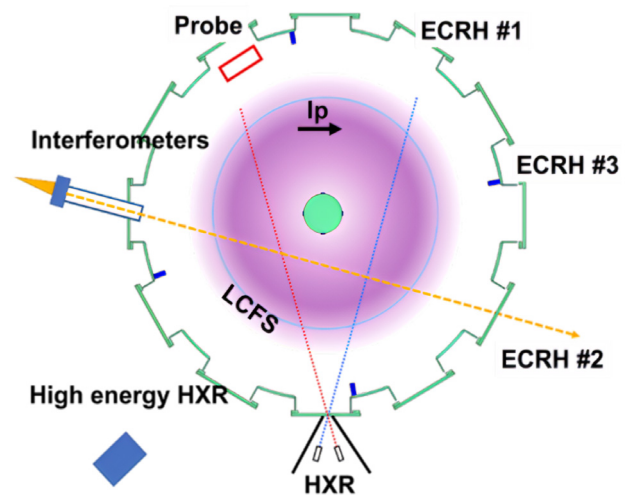


FIG. 1. A top-view diagram of EXL-50 is presented, with the location of the high-frequency magnetic probe, HXR diagnostic, high energy HXR detector, and three sets of ECW heating systems indicated.

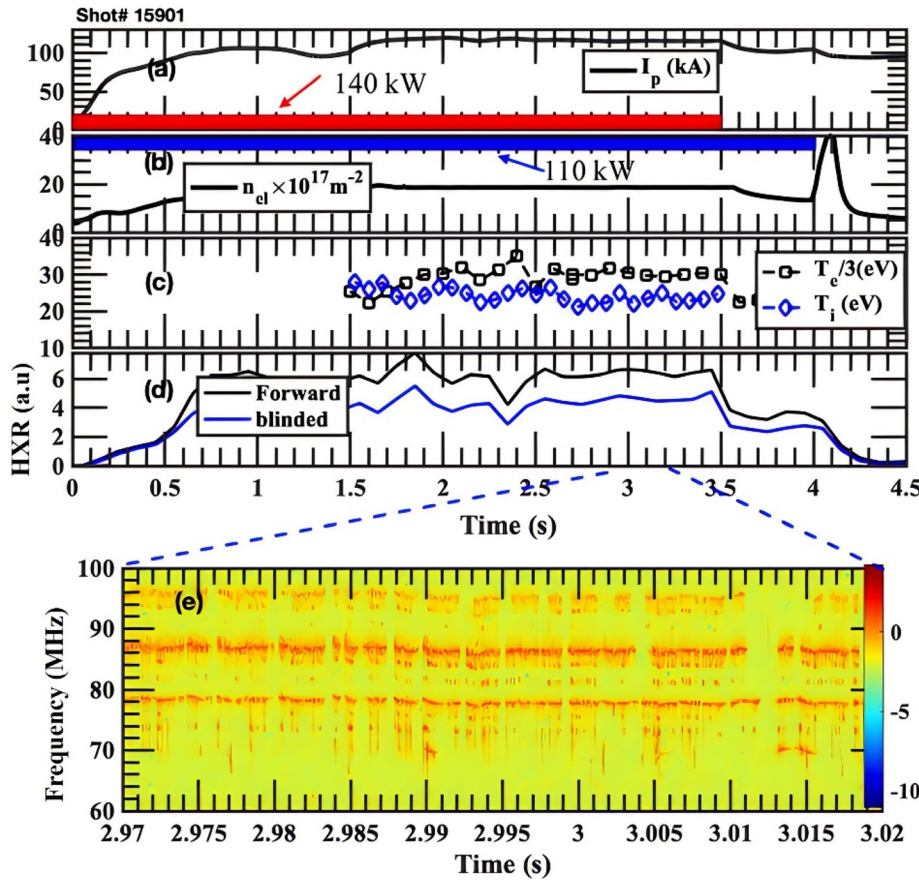


FIG. 2. Time evolution of (a) plasma current; (b) line integrated density; (c) temperature of electron (black dotted line) and ion (blue dotted line); (d) intensity of forward (black line) and blinded (blue line) HXR; and (e) magnetic fluctuation power spectra. Only ECW {140 kW [red bars in Fig. 2(a)] +110 kW [blue bars in Fig. 2(b)]} used to startup and maintain the plasma current.

{140 kW [red bars in Fig. 2(a)] +110 kW [blue bars in Fig. 2(b)]} used to startup and maintain the plasma current. The temperature of bulk electron (T_e) and ion (T_i) are around 90 and 20 eV, respectively. The forward (countercurrent) and blinded (without collimator) HXR detector measure similar intensities of HXR radiation. The intensity decreases significantly after the ECW is turned off. This suggests that the HXR detector measures mainly thick target radiation signal. Furthermore, the high-frequency electromagnetic rise and fall are measured by the high-frequency magnetic probe.

EXPERIMENTAL RESULTS AND ANALYSIS

The time evolution of magnetic fluctuation power spectra (a) and n_{cl} and B_T of typical ECRH discharges (b) is depicted in Fig. 3. Multiple coherent modes with frequencies ranging from 70 to 110 MHz (shot # 15033) and 30–120 MHz (shot # 14375) are observed. The frequency of the modes is observed to decrease gradually as the plasma density increases and the magnetic field strength decreases.

The parametric behavior of the whistler wave frequency can be understood through the dispersion relation in cold plasma, as outlined in the following equation:^{18,34}

$$\omega = kV_A \sqrt{1 + k_{\parallel}^2 c^2 / \omega_{pi}^2}, \quad (1)$$

where ω is the wave frequency, $V_A = B_T / \sqrt{4\pi n_e m_i}$ is the Alfvén velocity, n_e is the electron density, m_i is the ion mass, ω_{pi} is the ion plasma frequency, and k and k_{\parallel} are the total and component parallel to the magnetic field of the wave vector, respectively. For the lowest order ($k_{\parallel}^2 c^2 / \omega_{pi}^2 \sim 0$), Eq. (1) indicates a linear scaling of the frequency with Alfvén velocity ($\omega \propto V_A$) and an inverse square root scaling with the plasma density ($\omega \propto n_e^{-1/2}$).

These trends are confirmed with the results of density and magnetic field scanning experiments in Figs. 3(c) and 3(d), where mode frequency is clearly shown to be inversely proportional to the square root of the plasma density [Fig. 3(c)] and linearly proportional to the Alfvén velocity [Fig. 3(d)]. This suggests that these coherent modes are whistler waves.

According to Eq. (1), we can obtain

$$\frac{k_{\parallel} V_A \sqrt{1 + k_{\parallel}^2 c^2 / \omega_{pi}^2}}{\omega} < 1 \quad (2)$$

$$\frac{k_{\parallel} c}{\omega_{pi}} < \frac{m_i \omega c}{B_T e}.$$

Here, e is the elementary charge. There exists a region at the high field side where Eq. (2) is easier to be satisfied, so the whistler wave may be excited on the high field side on EXL-50.

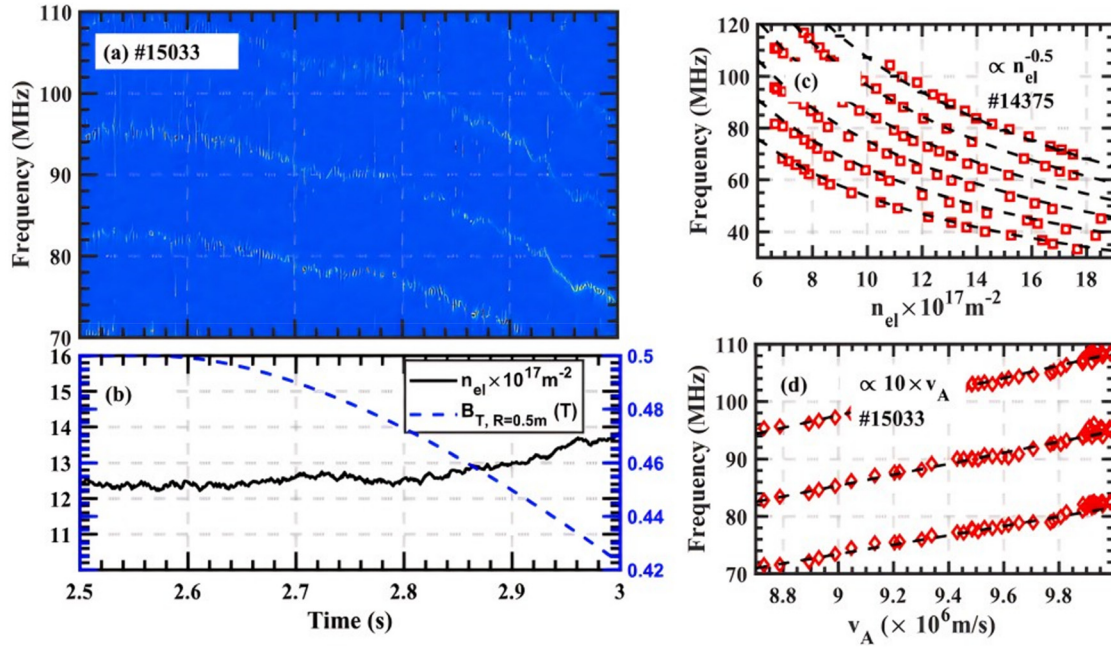


FIG. 3. Time evolution of (a) magnetic fluctuation power spectra and (b) toroidal magnetic field (near the magnetic axis) and line integrated density. Variation of mode frequency spectrum with line integrated density at constant toroidal magnetic field (c) and Alfvén velocity (d).

The anisotropy of the electron velocity distribution provides the energy that drives the whistler wave.^{18,35} Increasing the density of background electrons can serve to reduce the saturation intensity of the whistler wave by reducing the anisotropy of the energetic electron velocity distribution.^{36,37}

Here, we explore the correlation between the energy of saturated wave magnetic field and the bulk electron density. Figure 4 presents time evolution of the intensity and frequency of the whistler wave corresponding to the evolution of plasma density and the intensity of hard x-ray signal induced by fast electrons. As the plasma density

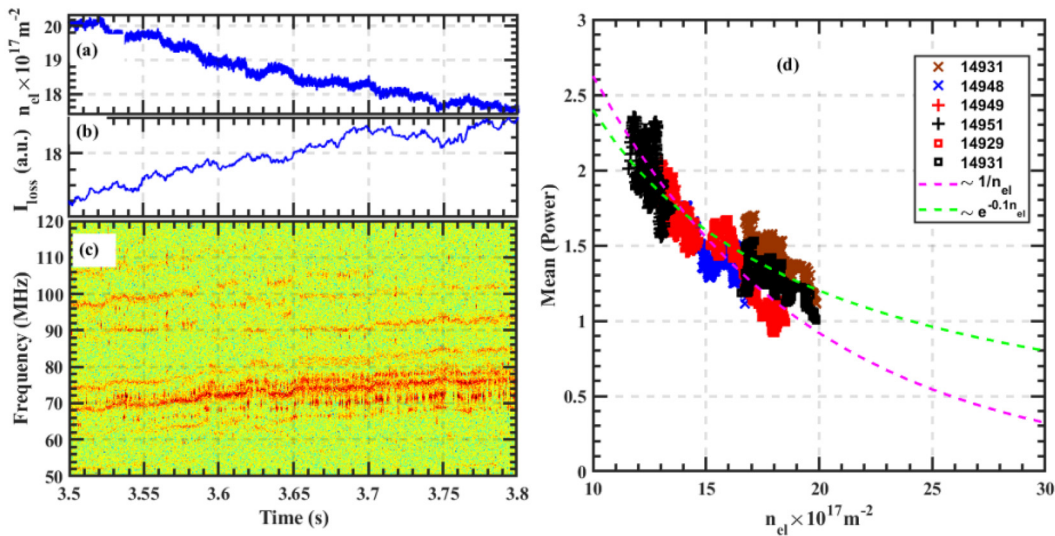


FIG. 4. Time evolution of (a) the line-integrated electron density, (b) distant hard x-ray signal, (c) whistler wave spectra, and (d) intensity of whistler wave fluctuations vs electron density, there is a threshold value of the electron density, triggering the whistler wave.

07 March 2024 08:37:25

decreases, the intensity and frequency of the whistler wave simultaneously increase. In Fig. 4(d), the dashed lines represent the fitted curves of $\frac{1}{n_d}$ and $\exp(-n_d/10)$, respectively. From the obtained results, it is evident that the whistler wave can be suppressed with an increase in density. It is noteworthy that energetic electrons are the primary carriers of EXL-50 plasma current, and the increase in plasma density leads to a decrease in the energetic electrons, and therefore, decreases in plasma current and the confinement. These further induce increasing of the loss of energetic electrons and cause the current to decrease further. This may account for the experimental challenge of observing the excitation of the whistler wave at densities higher than $2 \times 10^{18} \text{ m}^{-2}$. Finally, it is worth pointing out that the enhancement of whistler wave intensity is correlated with an increase in hard x-ray radiation induced by energetic electron loss (Fig. 3), indicating that the waves scatter energetic electrons into the loss phase space.^{38,39}

Currently, direct measurements of the parallel and perpendicular temperatures of energetic electrons are not available on EXL-50. Therefore, LHW was employed to change the anisotropy of the velocity distribution of energetic electrons. In shot 14970, LHW was turned on at 2.52 s, and shot 14971 served as a reference discharge without LHW. As shown in Fig. 5(a), the plasma current increased after the LHW activation in shot 14970, while the plasma current decreased continuously without the LHW in shot 14971. The plasma current is mainly carried by energetic electrons, and the increase in the plasma

current indicates an increase in the parallel energy of the electrons driven by the LHW.

Additionally, the distant HXR intensity is significantly reduced after the LHW activation [Fig. 5(b)], suggesting a reduction in energetic electron loss, which may be attributed to instability mitigation. The power spectrum of high-frequency fluctuation before and after LHW activation is compared [Fig. 5(c)]. The bands with frequency rise and fall (f_1, f_2, f_3 , and f_4) are completely suppressed, when LHW is activated, whereas the intensities of the bands with frequency rise and fall remain almost unchanged for shot 14971 [see Fig. 5(d)]. These results are consistent with the theoretical prediction when the energetic electrons have anisotropy of higher perpendicular temperature. It should be mentioned that not all whistler wave is suppressed, which may be related to the LHW deposition region.

Theoretical and experimental studies have demonstrated that scattering of whistler instability wave on electrons in homogeneous plasma can maintain the distribution of electrons near instability thresholds.² However, in toroidal plasma, the whistler wave may alter equilibrium by modifying the macroscopic properties (current and pressure) of the plasma. The ELMO Bumpy Torus exhibits a relatively low level of plasma current, and disruptions have been observed¹⁶ when the high-frequency hot electron instability is strongly excited.

As shown in Fig. 6, plasma current disruptions were observed. The radiation intensity induced by the loss of energetic electrons

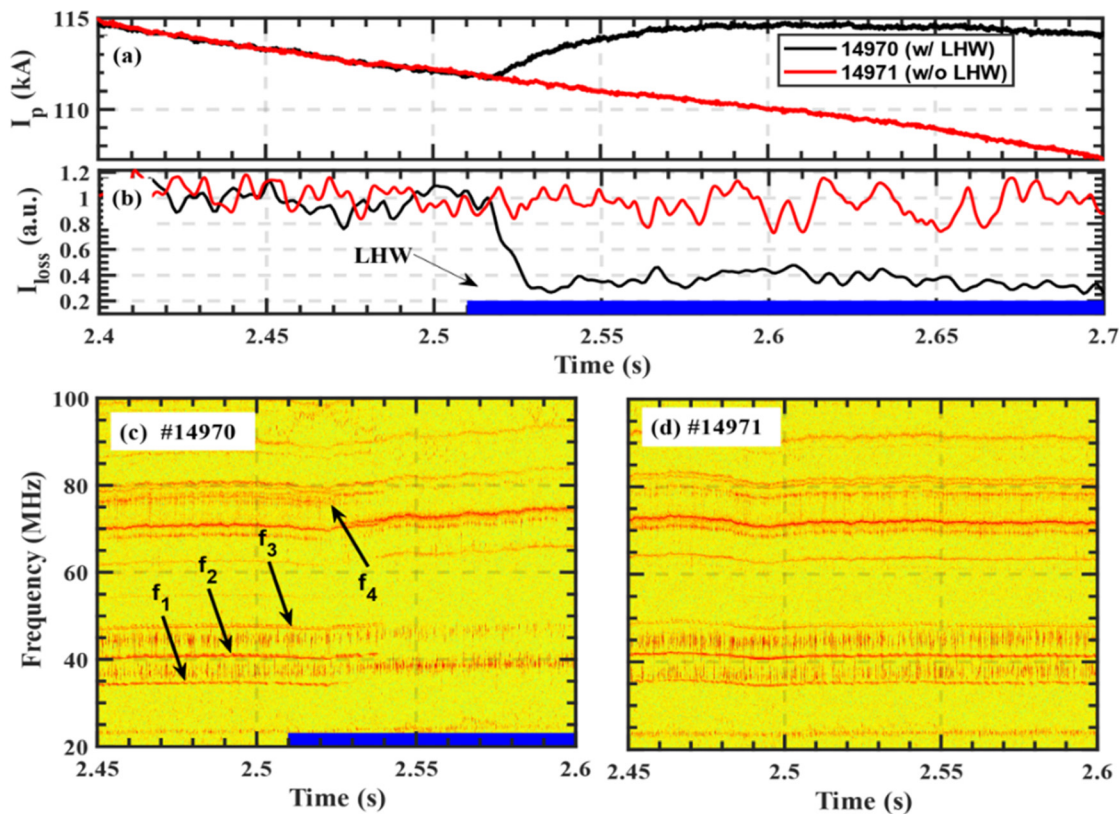


FIG. 5. Time evolution of (a) plasma current and (b) intensity of distant hard-x ray; comparison of (c) the power spectrum of the magnetic fluctuations of shot 14970 (with LHW) and (d) of shot 14971 (without LHW).

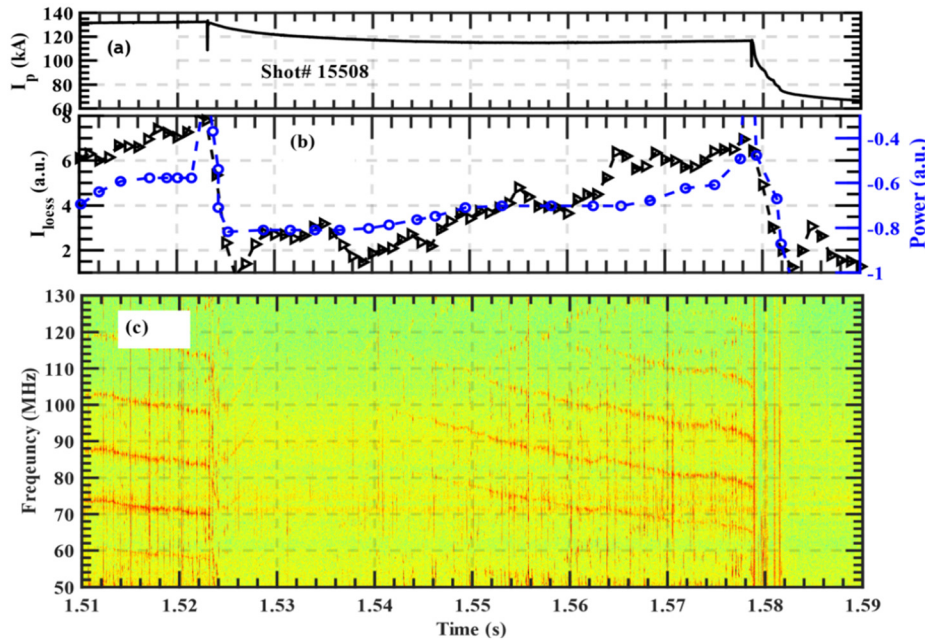


FIG. 6. The time evolution of (a) plasma current, (b) energetic electron loss intensity (black triangle) and whistler wave intensity (blue circle), and (c) the magnetic fluctuation power spectra.

increases with the whistler wave intensity, and current disruptions occur. These findings suggest that ECW may excite such waves and potentially limit the efficiency of current drive. Given that ECW non-inductive current drive is crucial for the advancement of spherical torus fusion devices, this is an issue that requires significant attention in ST.

DISCUSSION

Experiment and theory indicate that a stochastic wave can accelerate electrons to MeV energy at an input ECW power of a few 100 kW.^{23,40,41} These energetic electrons can lead to $\frac{\partial f}{\partial v_{\parallel}} > 0$ and $\frac{\partial f}{\partial v_{\parallel}} \neq 1$ (f is the electron distribution function) with the asymmetric structure of the confined energetic electron orbit on EXL-50,²⁴ both of which can provide free energy for generating whistler wave below $0.1\omega_{ce}$.^{7,35} The observed whistler wave instability may be driven when energetic electrons resonate with the wave.^{2,15,18} The resonance condition is

$$\omega - \mathbf{k}_{\parallel} \mathbf{v}_{\parallel} - k_{\perp} v_d - l\omega_{ce}/\gamma = 0. \quad (3)$$

Here, \mathbf{v}_{\parallel} is the parallel velocity of the electrons, k_{\perp} is the perpendicular component of the wave-vector, v_d is the orbital drift velocity, and γ is the relativistic factor. In the case of EXL-50, the observed wave frequency is much lower than the electron cyclotron frequency; therefore, $l = -1$ (Anomalous Doppler cyclotron resonance) or $l = 0$ (Landau resonance) resonances are relevant.

A three-fluid (bulk and energetic electrons and ions) equilibrium of EXL-50 plasma ($I_p = 123$ kA) with the multi-fluid equilibrium model⁴² is shown in Fig. 7. The bulk electron density is larger than the energetic electron density, and the plasma current is mainly carried by energetic electrons. The drift speed of energetic electrons is about $\sim 0.5c$. The effect of energetic electrons on plasma instability is

simulated by BO (“wave in Chinese”) code with the equilibrium parameters.⁴³ Here, $T_e \sim 110$ eV, $T_{\perp} = 200$ keV, $v_d = 0.5c$, $n_e = 0.1 \times 10^{18} \text{ m}^{-3}$, $\frac{n_{th}}{n_c} = 0.2$ ($R = 0.4$ m, $B_T = 0.6$ T, and $k = 6$), and the effect of bulk ions is neglected. The results are shown in Fig. 7. Low-frequency electromagnetic instabilities are excited in the frequency of 20–100 MHz with $k_z c/\omega_{pi} < 0.3$, and the growth rate of the instability is positively correlated with $\frac{T_{\perp}}{T_{\parallel}}$. The simulation results are qualitatively consistent with the experimental results. This provides one explanation for the experimental results.

ECW generates a large number of energetic electrons with energies exceeding MeV by stochastic heating. However, the experiments have not yet been able to distinguish the contribution of MeV energetic electrons to the excitation of the whistler wave via cyclotron resonance.

SUMMARY

This article presents an experimental study of whistler wave instability driven by energetic electrons in steady-state ECW plasma on a solenoid-free spherical torus. The study found that the frequency of the whistler wave is between 30 and 120 MHz and is proportional to the Alfvén velocity. The whistler wave intensity is verified to be correlated with the electron density and anisotropy of electron velocity distribution. In addition, the synergistic effect of LHW and ECW can suppress the whistler waves. The study also finds that plasma current disruptions occur in the spherical torus device with whistler. These findings suggest that ECW current-drive through the creation of energetic electrons may excite such waves, potentially limiting the efficiency of current drive.

The 100 kW ECW on EXL-50 can drive plasma currents of nearly 140 kA, often accompanied by whistler waves. Considering that RF also contributes to current drive, the study of whistler waves is of significant importance for understanding the physics of high-current

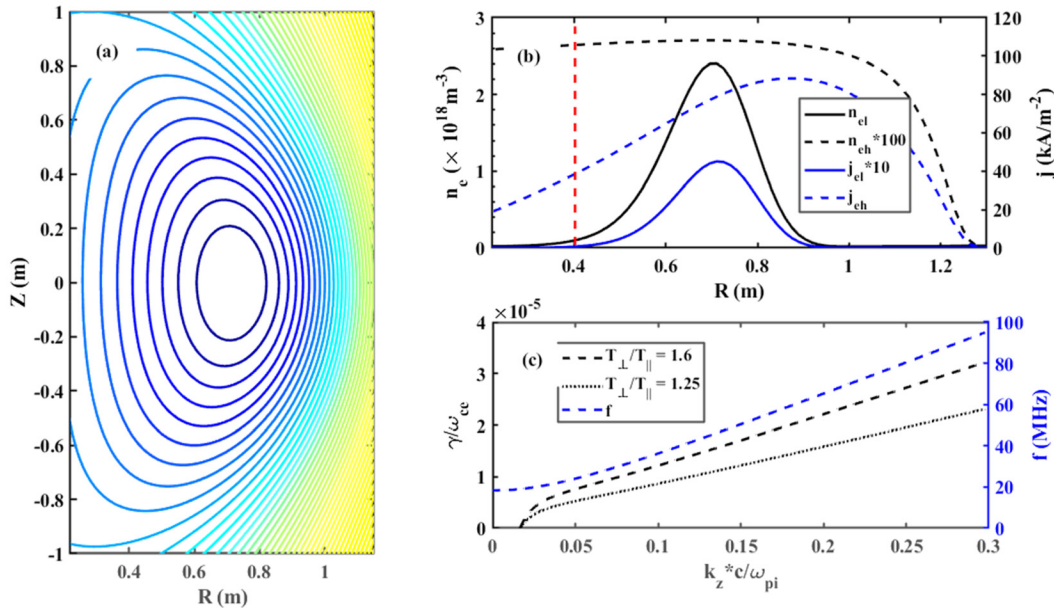


FIG. 7. (a) Contours of poloidal magnetic flux, (b) density and current profile of bulk electrons and energetic using multi-fluid plasma code, and (c) the growth rates and frequency of electromagnetic instabilities vs wave number.

drive in EXL-50 using ECW and for the application of high-current drive effects with ECW in other devices.

ACKNOWLEDGMENTS

The presented research was supported in part by the National Natural Science Foundation of China (Y.W., No. 12075284; G.Z., Grant No. U1967206; W.D., Grant No. 11975231; and W., Grant No. 11975273) and the Fundamental Research Funds for the Central Universities (Grant No. WK342000018). We acknowledge the ENN team for supporting the experiments.

AUTHOR DECLARATIONS

Conflict of Interest

The authors have no conflicts to disclose.

Author Contributions

Mingyuan Wang: Conceptualization (equal); Data curation (equal); Supervision (equal); Validation (equal); Visualization (equal); Writing – original draft (equal); Writing – review & editing (equal). **Yuejiang Shi:** Conceptualization (equal). **Jiaqi Dong:** Writing – review & editing (equal). **Xinliang Gao:** Conceptualization (lead); Formal analysis (equal). **Quanming Lu:** Data curation (equal); Formal analysis (lead). **Ziqi Wang:** Funding acquisition (lead); Investigation (equal). **Wei Chen:** Investigation (lead); Methodology (equal). **Adi Liu:** Supervision (equal); Validation (equal). **Ge Zhuang:** Data curation (equal); Writing – review & editing (equal). **Yumin Wang:** Validation (equal); Visualization (equal). **Shikui Cheng:** Data curation (equal); Formal analysis (supporting). **Mingsheng Tan:** Conceptualization (supporting); Writing – original draft (supporting); Writing – review & editing

(equal). **Songjian Li:** Data curation (equal); Validation (equal). **Shaodong Song:** Project administration (equal); Resources (equal). **Tiantian sun:** Investigation (equal); Software (supporting). **Bing Liu:** Resources (equal); Supervision (equal). **Xianli Huang:** Software (equal); Visualization (equal). **Yingying Li:** Data curation (equal); Software (supporting); Supervision (supporting). **Xianming Song:** Project administration (supporting); Resources (supporting). **Baoshan Yuan:** Visualization (equal); Writing – original draft (equal). **Y.-K. Martin Peng:** Supervision (equal); Validation (equal).

DATA AVAILABILITY

The data that support the findings of this study are available from the corresponding authors upon reasonable request.

REFERENCES

- ¹M. E. Mandt, R. E. Denton, and J. F. Drake, “Transition to whistler mediated magnetic reconnection,” *Geophys. Res. Lett.* **21**(1), 73–76, <https://doi.org/10.1029/93GL03382> (1994).
- ²S. P. Gary and J. Wang, “Whistler instability: Electron anisotropy upper bound,” *J. Geophys. Res.* **101**(A5), 10749–10754, <https://doi.org/10.1029/96JA00323> (1996).
- ³R. L. Stenzel, “Whistler waves in space and laboratory plasmas,” *J. Geophys. Res.* **104**(A7), 14379–14395, <https://doi.org/10.1029/1998JA900120> (1999).
- ⁴S. Galtier and A. Bhattacharjee, “Anisotropic weak whistler wave turbulence in electron magnetohydrodynamics,” *Phys. Plasmas* **10**(8), 3065–3076 (2003).
- ⁵N. P. Meredith, R. B. Horne, W. Li, R. M. Thorne, and A. Sicard-Piet, “Global model of low-frequency chorus ($f_{LHR} < f < 0.1 f_{ce}$) from multiple satellite observations,” *Geophys. Res. Lett.* **41**(2), 280–286, <https://doi.org/10.1002/2013GL059050> (2014).
- ⁶C. A. Cattell, A. W. Breneman, S. A. Thaller, J. R. Wygant, C. A. Kletzing, and W. S. Kurth, “Van Allen Probes observations of unusually low frequency whistler mode waves observed in association with moderate magnetic storms: Statistical study,” *Geophys. Res. Lett.* **42**(18), 7273–7281, <https://doi.org/10.1002/2015GL065565> (2015).

- ⁷F. Xiao, S. Liu, X. Tao, Z. Su, Q. Zhou, C. Yang, Z. He, Y. He, Z. Gao, D. N. Baker *et al.*, "Generation of extremely low frequency chorus in Van Allen radiation belts," *J. Geophys. Res.* **122**(3), 3201–3211, <https://doi.org/10.1002/2016JA023561> (2017).
- ⁸C. Kennel, "Low-frequency whistler mode," *Phys. Fluids* **9**(11), 2190–2202 (1966).
- ⁹R. W. Boswell, "Very efficient plasma generation by whistler waves near the lower hybrid frequency," *Plasma Phys. Controlled Fusion* **26**(10), 1147 (1984).
- ¹⁰R. C. Garner, A. M. Mauel, R. S. Post, and D. L. Smatlak, "Warm electron-driven whistler instability in an electron-cyclotron-resonance heated, mirror-confined plasma," *Phys. Rev. Lett.* **59**(16), 1821 (1987).
- ¹¹C. Krafft and M. Starodubtsev, "Whistler excitation by electron beams in laboratory plasmas," *Planet. Space Sci.* **50**(2), 129–149 (2002).
- ¹²R. L. Stenzel, J. M. Urrutia, and K. D. Strohmaier, "Whistler instability in an electron-magnetohydrodynamic spheromak," *Phys. Rev. Lett.* **99**(26), 265005 (2007).
- ¹³B. Van Compernelle, J. Bortnik, P. Pribyl, W. Gekelman, M. Nakamoto, X. Tao, and R. M. Thorne, "Direct detection of resonant electron pitch angle scattering by whistler waves in a laboratory plasma," *Phys. Rev. Lett.* **112**(14), 145006 (2014).
- ¹⁴D. A. Spong, W. W. Heidbrink, C. Paz-Soldan, X. D. Du, K. E. Thome, M. A. Van Zeeland, C. Collins, A. Lvovskiy, R. A. Moyer, M. E. Austin *et al.*, "First direct observation of runaway-electron-driven whistler waves in tokamaks," *Phys. Rev. Lett.* **120**(15), 155002 (2018).
- ¹⁵A. Lvovskiy, W. W. Heidbrink, C. Paz-Soldan, D. A. Spong, A. Dal Molin, N. W. Eidietis, M. Nocente, D. Shiraki, and K. E. Thome, "Observation of rapid frequency chirping instabilities driven by runaway electrons in a tokamak," *Nucl. Fusion* **59**(12), 124004 (2019).
- ¹⁶S. Hiroe, J. B. Wilgen, F. W. Baitty, L. A. Berry, R. J. Colchin, W. A. Davis, A. M. El Nadi, G. R. Haste, D. L. Hillis, D. A. Spong *et al.*, "Observation of hot electron ring instabilities in ELMO Bumpy Torus," *Phys. Fluids* **27**(4), 1019–1029 (1984).
- ¹⁷W. W. Heidbrink, C. Paz-Soldan, D. A. Spong, X. D. Du, K. E. Thome, M. E. Austin, A. Lvovskiy, R. A. Moyer, R. I. Pinsky, and M. A. Van Zeeland, "Low-frequency whistler waves in quiescent runaway electron plasmas," *Plasma Phys. Controlled Fusion* **61**(1), 014007 (2018).
- ¹⁸T. Fülöp, G. Pokol, P. Helander, and M. Lisak, "Destabilization of magnetosonic-whistler waves by a relativistic runaway beam," *Phys. Plasmas* **13**(6), 062506 (2006).
- ¹⁹Y. A. Sokolov, "'Multiplication' of accelerated electrons in a tokamak," *JETP Lett.* **29**(4), 218–221 (1979).
- ²⁰C. Liu, E. Hirvijoki, G. Y. Fu, D. P. Brennan, A. Bhattacharjee, and C. Paz-Soldan, "Role of kinetic instability in runaway-electron avalanches and elevated critical electric fields," *Phys. Rev. Lett.* **120**(26), 265001 (2018).
- ²¹B. N. Breizman, P. Aleynikov, E. M. Hollmann, and M. Lehnen, "Physics of runaway electrons in tokamaks," *Nucl. Fusion* **59**(8), 083001 (2019).
- ²²Z. Guo, C. J. McDevitt, and X. Z. Tang, "Control of runaway electron energy using externally injected whistler waves," *Phys. Plasmas* **25**(3), 032504 (2018).
- ²³M. Wang, S. Cheng, B. Liu, S. Song, D. Guo, Y. Song, W. Liu, D. B. J. Li, T. Sun *et al.*, "Generation of energetic electrons by an electron cyclotron wave through stochastic heating in a spherical tokamak," *J. Plasma Phys.* **89**(6), 905890603 (2023).
- ²⁴Y. Shi, B. Liu, S. Song, Y. Song, X. Song, B. Tong, S. Cheng, W. Liu, M. Wang, T. Sun *et al.*, "Solenoid-free current drive via ECRH in EXL-50 spherical torus plasmas," *Nucl. Fusion* **62**(8), 086047 (2022).
- ²⁵X. Tang, C. Cattell, J. Dombeck, L. Dai, L. B. Wilson, A. Breneman, and A. Hupach, *Geophys. Res. Lett.* **40**, 2884, <https://doi.org/10.1002/grl.50565> (2013); C. A. Cattell *et al.*, *Geophys. Res. Lett.* **29**, 1065 (2002).
- ²⁶X. Deng, M. Ashour-Abdalla, M. Zhou, R. Walker, M. El-Alaoui, V. Angelopoulos, R. E. Ergun, and D. Schriver, *J. Geophys. Res.* **115**, A09225, <https://doi.org/10.1029/2009JA015107> (2010).
- ²⁷Cerenkov Emission of Quasiparallel Whistlers by Fast Electron Phase-Space Holes during Magnetic Reconnection.
- ²⁸S. J. Li, R. H. Bai, R. Y. Tao, N. Li, X. C. Lun, L. C. Liu, Y. Liu, M. S. Liu, and B. H. Deng, "A quasioptical microwave interferometer for the XuanLong-50 experiment," *J. Instrum.* **16**(8), T08011 (2021).
- ²⁹M. Wang, D. Guo, Y. Shi, B. Chen, B. Liu, S. Song, X. Zhao, Y. Song, W. Liu, Y. Guan *et al.*, "Experimental study of non-inductive current start-up using electron cyclotron wave on EXL-50 spherical torus," *Plasma Phys. Controlled Fusion* **64**, 075006 (2022).
- ³⁰S. L. Ossakow, I. Haber, and E. Ott, "Simulation of whistler instabilities in anisotropic plasmas," *Phys. Fluids* **15**(8), 1538–1540 (1972).
- ³¹H. P. Kim, J. Hwang, J. J. Seough, and P. H. Yoon, "Electron temperature anisotropy regulation by whistler instability," *J. Geophys. Res.* **122**(4), 4410–4419, <https://doi.org/10.1002/2016JA023558> (2017).
- ³²M. Wang, X. Lun, X. Bo, B. Liu, A. Liu, and Y. Shi, "Radio-frequency measurements of energetic-electron-driven emissions using high-frequency magnetic probe on XuanLong-50 spherical torus," *Plasma Sci. Technol.* **25**, 045104 (2022).
- ³³S. K. Cheng, Y. B. Zhu, Z. Y. Chen, Y. X. Li, R. H. Bai, B. Chen, X. L. Huang, L. L. Dai, and M. S. Liu, "Tangential hard x-ray diagnostic array on the EXL-50 spherical tokamak," *Rev. Sci. Instrum.* **92**(4), 043513 (2021).
- ³⁴G. Pokol, T. Fülöp, and M. Lisak, "Quasi-linear analysis of whistler waves driven by relativistic runaway beams in tokamaks," *Plasma Phys. Controlled Fusion* **50**(4), 045003 (2008).
- ³⁵S. Wang, N. Bessho, D. B. Graham, O. Le Contel, F. D. Wilder, Y. V. Khotyaintsev, K. J. Genestreti, B. Lavraud, S. Choi, J. L. Burch *et al.*, "Whistler waves associated with electron beams in magnetopause reconnection diffusion regions," *J. Geophys. Res.* **127**(9), e2022JA030882, <https://doi.org/10.1029/2022JA030882> (2022).
- ³⁶E. G. Harris, "Physics of hot plasmas," *Plasma Instability* (Oliver and Boyd, Edinburgh, 1970), Chap. 4, p. 158.
- ³⁷D. Maslovsky, B. Levitt, and M. E. Mauel, "Observation of nonlinear frequency-sweeping suppression with RF diffusion," *Phys. Rev. Lett.* **90**(18), 185001 (2003).
- ³⁸S. P. Gary and H. Karimabadi, "Linear theory of electron temperature anisotropy instabilities: Whistler, mirror, and Weibel," *J. Geophys. Res.* **111**, 11224, <https://doi.org/10.1029/2006JA011764> (2006).
- ³⁹S. P. Gary, D. Winske, and M. Hesse, "Electron temperature anisotropy instabilities: Computer simulations," *J. Geophys. Res.* **105**(A5), 10751–10759, <https://doi.org/10.1029/1999JA000322> (2000).
- ⁴⁰H. Ikegami, S. Aihara, M. Hosokawa, and H. Aikawa, *Nucl. Fusion* **13**, 351 (1973).
- ⁴¹P. A. Sturrock, *Phys. Rev.* **141**, 186 (1966).
- ⁴²A. Ishida, Y. K. M. Peng, and W. Liu, "Four-fluid axisymmetric plasma equilibrium model including relativistic electrons and computational method and results," *Phys. Plasmas* **28**(3), 032503 (2021).
- ⁴³H. Xie, "BO: A unified tool for plasma waves and instabilities analysis," *Comput. Phys. Commun.* **244**, 343–371 (2019).